

Effective potentials for quarkonium above deconfinement

K. Dusling* and C. Young†

*Department of Physics & Astronomy, State University of New York,
Stony Brook, NY 11794-3800, U.S.A.*

(Dated: April 19, 2019)

Abstract

Using methods previously developed by Kelbg and others for creating effective potentials for electron-ion plasmas, we investigate quarkonium potentials above deconfinement. Using lattice results for the free energy of a static quark-antiquark ($Q\bar{Q}$) pair, a set of effective potentials are constructed that take into account quantum effects and symmetry conditions. Bound state effects are explicitly included in order to account for the strongly coupled nature of the plasma. It is hoped that these effective potentials will be useful in simulations of heavy quarks or plasma quasiparticles when the dynamics is treated classically.

PACS numbers:

*Electronic address: kdusling@ic.sunysb.edu

†Electronic address: cyoung@grad.physics.sunysb.edu

I. INTRODUCTION

It has recently been noted that the matter produced in heavy ion collisions at RHIC cannot be weakly coupled but instead behaves as a good liquid [1, 2]. The evidence for the sQGP is large but mainly consists of the following two points: 1. the observed collective flows at RHIC can be explained by hydrodynamics showing that the dissipative lengths are very short and 2. binary bound states are seen to exist in lattice simulations above T_c and are also predicted [3] using lattice interparticle potentials.

Since a complete quantum description tends to rely on perturbative methods other approaches have to be adopted in order to perform calculations at strong coupling. One approach as was first discussed in [4, 5], is to model the strongly interacting quark and gluon quasiparticles as a classical non-relativistic colored Coulomb gas. This model is analyzed using molecular dynamics (MD) simulations in which real time correlators can be extracted. The interaction between quarks was taken as a Coulomb potential with a strong repulsive core in order to *mock up* quantum-mechanical effects.

A second example is a model treating charmonium in the sQGP [6], where initial ensembles of quark pairs from pQCD events are evolved classically according to a Langevin model with an additional interaction potential included between quark-antiquark pairs. The interaction potential was taken from lattice $c\bar{c}$ internal energy data with quantum-mechanical effects mimicked by simply turning off the potential below the approximate Bohr radius.

If these models are to be refined it is necessary that we consider quantum-mechanical effects more carefully. The goal of this work is to generate classical effective $q\bar{q}$ potentials which take into account quantum-mechanical effects. We want to find an effective potential $V_{eff}(\vec{r}, T)$ whose *classical* Boltzmann factor yields the diagonal term of the *quantum – mechanical* density matrix:

$$\langle \vec{r} | e^{-\beta \hat{H}} | \vec{r} \rangle = e^{-\beta V_{eff}(\vec{r}, T)} \langle \vec{r} | e^{-\frac{\hat{p}^2}{2m}} | \vec{r} \rangle \quad (1)$$

For example, if this corrected interaction were used in the modeling of charmonium discussed in the previous paragraph, the final equilibrium distribution obtained by the Fokker-Planck evolution would be the correct quantum-mechanical distribution. This would obviously improve estimates for the intermediate states as well. These effective interactions would also have use in the MD simulations discussed earlier.

In this work we calculate effective quark-antiquark potentials from lattice calculations of the internal energy of static $Q\bar{Q}$ pairs measured in [7]. Section II of this paper summarizes a number of previous works [8, 9, 10, 11], including the definition of the Slater sum and its use in creating effective potentials. The original results of this paper start in section III, where the methods presented in section II are applied to potentials extracted from lattice data.

II. CREATING EFFECTIVE POTENTIALS

A. The Slater Sum

Anticipating applications of this work to many-particle systems, we define the N -particle Slater sum:

$$S^{(N)}(\vec{r}_1, \dots, \vec{r}_N) = N! \Lambda^{3N} \sum_i |\Psi_i(\vec{r}_1, \dots, \vec{r}_N)|^2 e^{-\beta E_i} \quad (2)$$

where Ψ_i are the N -particle energy eigenfunctions and $\Lambda = \sqrt{\frac{h^2}{2\pi m k T}}$ is the thermal wavelength. Integrating the Slater sum in coordinate space yields the partition function:

$$Z = \frac{1}{N! \Lambda^{3N}} \int (d\vec{r}_1 \dots d\vec{r}_N) S^{(N)}(\vec{r}_1, \dots, \vec{r}_N) \quad (3)$$

In the case of ideal particles using Boltzmann statistics the partition function is given as $Z_{MB} = \frac{V^N}{N! \Lambda^{3N}}$. The corresponding free energy can then be separated in the following way:

$$F = -k_B T \ln Z = F_{MB} - k_B T \ln \frac{Z}{Z_{MB}} \quad (4)$$

Substituting eq. 3 for Z in the above equation yields:

$$F = F_{MB} - k_B T \ln \frac{1}{V^N} \int (d\vec{r}_1 \dots d\vec{r}_N) S^{(N)}(\vec{r}_1, \dots, \vec{r}_N) \quad (5)$$

This expression should now be compared to the classical counterpart of the free energy:

$$F = F_{MB} - k_B T \ln \frac{1}{V^N} \int (d\vec{r}_1, \dots, d\vec{r}_N) e^{-\beta \sum_{i < j} V_{ij}} \quad (6)$$

In the classical limit one obtains:

$$S^{(N)}(\vec{r}_1, \dots, \vec{r}_N) = e^{-\beta \sum_{i<j} V_{ij}} \quad (7)$$

and near the classical limit one can include multi-body interactions due to the quantum correlations between particles:

$$S^{(N)}(\vec{r}_1, \dots, \vec{r}_N) = e^{-\beta \sum_{i<j} u_{ij} - \beta \sum_{i<j<k} u_{ijk} + \dots} \quad (8)$$

where u_{ij} and u_{ijk} are effective two- and three-body interactions respectively and can be expressed in terms of two- and three-particle Slater sums as:

$$\begin{aligned} u_{ij} &= -k_B T \ln S^{(2)}(r_i, r_j) \\ u_{ijk} &= -k_B T \ln \frac{S^{(3)}(r_i, r_j, r_k)}{S^{(2)}(r_i, r_j) S^{(2)}(r_i, r_k) S^{(2)}(r_j, r_k)} \end{aligned} \quad (9)$$

Keeping only the first term, u_{ij} , in the series for $S^{(N)}$ accounts for quantum effects up to first order in the coupling parameter, $\Gamma = \frac{(Ze)^2}{a_{WS} T}$ where Ze, a_{WS}, T are respectively the ion charge, the Wigner-Seitz radius $a_{WS} = (3/4\pi n)^{1/3}$ and the temperature. The second term u_{ijk} introduces corrections to the effective potential of order Γ^2 .

B. Effective potentials in the binary approximation

The previous section motivates us to take the binary approximation:

$$S^{(N)} \approx e^{-\beta u_{ij}} \quad (10)$$

where u_{ij} is defined as in eq. 9. This approximation is exact for a 2-body systems (for example the model discussed in section I where a heavy quark only interacts with its diagonal partner). For the remainder of this paper, we now focus on an explicit calculation of u_{ij} . Our method involves examining the two-particle density matrix:

$$\rho(\vec{r}_1, \vec{r}_2, \vec{r}'_1, \vec{r}'_2) = \sum_i \Psi_i^*(\vec{r}_1, \vec{r}_2) \Psi_i(\vec{r}'_1, \vec{r}'_2) e^{-\beta E_i} \quad (11)$$

where the diagonal term is proportional to the needed Slater sum. The two-particle density matrix can then be factored into center-of-mass and relative components, $\rho(\vec{r}_1, \vec{r}_2, \vec{r}'_1, \vec{r}'_2) = \rho(\vec{R}, \vec{R}') \rho(\vec{r}, \vec{r}')$.

The two-body effective potential can then be found in the limit as $\vec{R}' \rightarrow \vec{R}$ and $\vec{r}' \rightarrow \vec{r}$. Since $\rho(\vec{R}, \vec{R}) = 1$ one is left with solving for $\rho(\vec{r}, \vec{r})$.

Acting on $\rho(\vec{r}, \vec{r}')$ with the one-particle Hamiltonian¹, $H = -\frac{1}{2m}\nabla^2 + V(\vec{r})$ where $m^{-1} = m_1^{-1} + m_2^{-1}$ is the reduced mass of the two particle system and \vec{r} is the relative coordinate it can be shown that ρ satisfies:

$$H\rho = -\frac{\partial\rho}{\partial\beta} \quad (12)$$

The boundary condition on the density matrix is given from the fact that $\{\Psi_i\}$ is a complete basis: $\rho(\vec{r}, \vec{r}'; \beta = 0) = \delta(\vec{r} - \vec{r}')$

We use the same method of solution on eq. 12 which is given in [8]. The solution to the free-particle density matrix ($V=0$ in eq. 12) is given as

$$\rho_0(\vec{r}, \vec{r}', \beta) = \frac{1}{(\sqrt{4\pi\lambda})^3} \exp\left(\frac{-|\vec{r} - \vec{r}'|^2}{4\lambda^2}\right) \quad (13)$$

where $\lambda = \sqrt{\frac{1}{2mT}}$ and m is the reduced mass of the two-particle system.

We then define the effective potential as in the introduction:

$$\rho(\vec{r}, \vec{r}', \beta) = \rho_0 e^{-\beta u(\vec{r}, \vec{r}', \beta)} \quad (14)$$

The effective two body potential u_{ij} of interest is simply the diagonal part of $u(\vec{r}, \vec{r}', \beta)$ when $\vec{r}' = \vec{r}$.

Substituting the above form for the density matrix into the Bloch equation 12 one finds that $u(\vec{r}, \vec{r}', \beta)$ satisfies:

$$\frac{1}{2m}\beta\nabla^2 u - \frac{1}{2}\beta^2(\nabla u)^2 - (\vec{r} - \vec{r}') \cdot \nabla u + V(\vec{r}) = \beta(\partial u / \partial \beta) + u \quad (15)$$

In the limit that u , $\nabla_r u$, or β is small, eq. 15 may be linearized:

$$\frac{1}{2m}\beta\nabla^2 u_1 - (\vec{r} - \vec{r}') \cdot \nabla u_1 + V(\vec{r}) = \beta(\partial u_1 / \partial \beta) + u_1 \quad (16)$$

the solution of which we call $u_1(\vec{r}, \vec{r}', \beta)$. As has been emphasized in [8], this condition is far more permissive than the typical condition from perturbation theory that u be small. This equation can be solved exactly:

$$u_1(\vec{r}, \vec{r}') = \int d\vec{r}_1 G(\vec{r}\vec{r}', \vec{r}_1, \beta) \quad (17)$$

¹ From here on we use standard high-energy units where $\hbar = c = 1$

where the Green function G is given by

$$G(\vec{r}\vec{r}', \vec{r}_1, \beta) = \frac{m}{2\pi\beta} \exp\left(-\frac{m|\vec{r} - \vec{r}'|^2}{2\beta}\right) \left[\frac{|\vec{r} - \vec{r}_1| - |\vec{r}' - \vec{r}_1|}{|\vec{r} - \vec{r}_1| |\vec{r}' - \vec{r}_1|} \right] \exp\left(-\frac{m(|\vec{r} - \vec{r}_1| + |\vec{r}' - \vec{r}_1|)^2}{2\beta}\right) \quad (18)$$

For a spherically symmetric potential $V(\vec{r})$, the angular integration in the above equation can be performed and the final result for the diagonal term is given as $u_1(\vec{r} = \vec{r}', \beta)$ is

$$u_1(\vec{r}, \beta) = \frac{1}{\lambda} \sqrt{\frac{\pi}{4}} \int_0^\infty \frac{r_1}{r} V(r_1) \left[\operatorname{erf}\left(\frac{|r + r_1|}{\lambda}\right) - \operatorname{erf}\left(\frac{|r - r_1|}{\lambda}\right) \right] dr_1 \quad (19)$$

Equation 19 will be the starting point for our future analysis of lattice potentials. It can be shown that the same result can be found by solving for the Slater sum $S^{(2)}$ explicitly using plane waves for the wavefunction and solving perturbatively in the coupling constant. It has already been shown in [8] that the approximation done in eq. 16 is satisfactory assuming the contribution due to bound states is small. In order to explicitly take into account the effect of bound states we follow [9] whereby the partition function is split up into a free part and a bound state part:

$$S^{(2)}(r, \beta) = (1 - P')S^{(2)} + P'S^{(2)} \quad (20)$$

The operator P' projects out the bound state components of the two-particle Slater sum. Using the Brillouin-Planck-Larkin (BPL) convention it becomes

$$P' \sum_i e^{-\beta E_i} = \sum_i [e^{-\beta E_i} - 1 + \beta E_i] \quad (21)$$

This leads to the following equation for the two-particle Slater sum:

$$S^{(2)}(r, \beta) = S_f^{(2)}(r, \beta) + \sum_i |\Psi_i(r)|^2 [e^{-\beta E_i} - 1 + \beta E_i] \quad (22)$$

where $S_f^{(2)}(r, \beta)$ is the free-particle Slater sum and can be found by substituting the result from eq. 19 into eq. 9. The second term includes a sum over bound states only.

We make one final consideration in creating effective potentials: symmetry conditions for identical particles. In the case of the identical fermions, the two-particle density matrix, written as an imaginary-time propagator, becomes

$$\rho(\vec{r}_1, \vec{r}_2, \vec{r}'_1, \vec{r}'_2, \beta) = \frac{1}{2} (\langle \vec{r}_1, \vec{r}_2 | - \langle \vec{r}_2, \vec{r}_1 |) \exp(-\beta \hat{H}) (|\vec{r}'_1, \vec{r}'_2\rangle - |\vec{r}'_2, \vec{r}'_1\rangle) \quad (23)$$

For our situation where two particles interact according to a potential only dependent on $|\vec{r}|$, their relative separation, this formula dramatically simplifies:

$$\rho(\vec{r}_1, \vec{r}_2, \vec{r}'_1, \vec{r}'_2, \beta) = \rho_{abs}(\vec{R}, \vec{R}', \beta) [\rho_{rel}(\vec{r}, \vec{r}', \beta) - \rho_{rel}(\vec{r}, -\vec{r}', \beta)] \quad (24)$$

Again, we will be interested in the limit $\vec{r}' = \vec{r}$. We may calculate explicitly the off-diagonal term of the density matrix needed in eq. 24, or we may follow the approach in [10] and approximate the off-diagonal term using only the off diagonal free particle density matrix

$$\rho_{rel}(\vec{r}, -\vec{r}, \beta) \approx \exp(-2m|\vec{r}|^2/\beta) \rho_{rel}(\vec{r}, \vec{r}, \beta) \quad (25)$$

The final form for the correctly symmetrized density matrix ρ_{sym} is given as:

$$\rho_{sym}(\vec{r}, \beta) = \frac{1}{\lambda^3} [1 \pm \exp(-2m|\vec{r}|^2/\beta)] e^{-\beta u_1(\vec{r})} \quad (26)$$

where a minus sign is used for fermions and a plus sign is for bosons.

C. Coulomb Potential

We now apply the methods outlined in the previous section to the case of the Coulomb potential. We first note that equation 19 can be integrated exactly in the case of a Coulomb potential, $V(r) = -1/r$ with the result:

$$u_1(r, \beta) = \frac{-1}{r} \left(1 - e^{-r^2/\lambda^2} + \frac{\sqrt{\pi}r}{\lambda} \left[1 - \operatorname{erf}\left(\frac{r}{\lambda}\right) \right] \right) \quad (27)$$

In figure II C we show the results of including bound states for the case of the Coulomb potential. The dotted green and blue curves show the results for $u_1(r)$ for values of $\beta = 10$ and 1 respectively. The corresponding solid curves show the results of including the first lowest bound state in the sum in eqn 22. The solid red curve shows the result at $\beta = \infty$ where the result u_1 vanishes but the effective potential sits at the energy of the lowest bound state $E_1 = -\frac{1}{2}$ in atomic units.

Also shown on this plot (black triangles) are numerical results of a Monte-Carlo simulation of the density matrix. Paths in imaginary time were sampled from the free-particle distribution by way of the Levy construction, and the actions of these paths were calculated and averaged according to their weights determined from the sampled, free-particle distribution of paths. See Ceperley [12] for an extremely useful and pedagogical introduction into Monte-Carlo methods for calculating N -particle (Bose) density matrices.

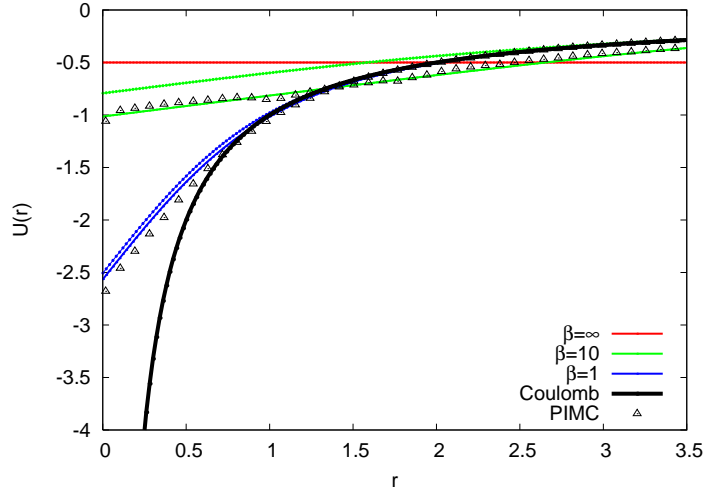


FIG. 1: Effective Coulomb potential for $\beta = 1, 10$. Dotted lines show the Kelbg potential $u_1(r)$ and corresponding solid line shows potential including correction from lowest bound state. The triangles are the results of PIMC (see text).

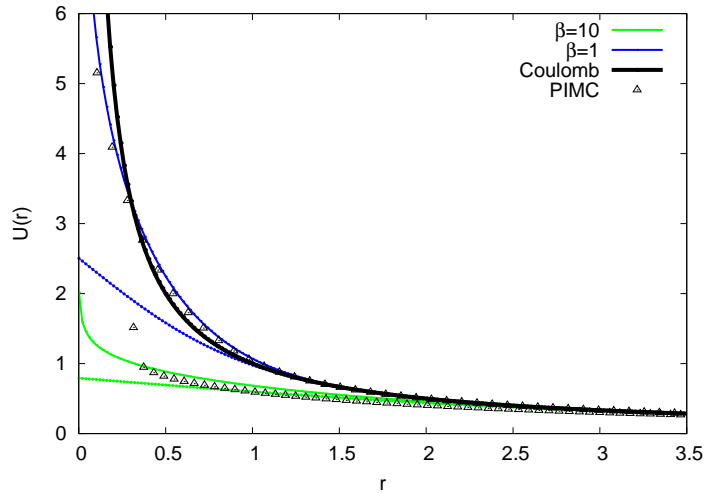


FIG. 2: Dotted lines show the Kelbg potential for a repulsive electron pair. The solid lines show the potential after anti-symmetrization of the density matrix. The triangles are the results of the PIMC.

In fig 2 we show the result for two identical electrons after the correct symmetrization is preformed. Again the dotted lines show the result of u_1 and the corresponding solids lines are the result after anti-symmetrization of the density matrix 26.

III. EFFECTIVE LATTICE POTENTIALS

A. Lattice Parameterization

We parameterize the free energy in the temperature range $1.1 - 2T_C$ using the following parameterization:

$$E_1(r, T) = -\frac{\alpha(T)}{r} e^{-\mu(T)r} + \frac{\sigma(T)}{b} \tanh(a\mu(T)r) \quad (28)$$

This potential is similar in form to the screened Cornell potential as first proposed in [13]. The first part of the potential is the usual screened Coulomb potential with temperature dependent coupling (α) and Debye mass (μ). These values were extracted from the lattice data and parameterized as follows. For the coupling constant we use a form similar to that from the leading log order RGE, $\alpha(T) = [2.4 \ln(2T/T_c)]^{-1}$. The fit to the Debye mass goes as $\mu \propto T$ which is consistent with the lowest-order perturbative calculations [14] with additional corrections to account for the data better: $\mu(T) = 0.0675(T/T_c) - (\frac{0.196T}{T_c})^5$.

The second part of the potential takes on the same form as a screened linear confining potential. We choose a different functional form than the usual $\sigma r e^{-\mu r}$ in order that the potential remains flat at intermediate and large distances instead of having a maximum and then becoming repulsive at larger r as in the case of the Cornell potential. We find that a parameterization of the *string tension* as $\sigma(T)/(\text{GeV}^2) = 0.32(T_c/T) + 0.8(T_c/T)^{16} + 0.005$ reproduces the lattice data reasonably well across a large range of temperatures. The final parameters are $a = 5.5, b = 0.37 \text{ GeV}$ and $T_c = 0.27 \text{ GeV}$.

The potential is then given as:

$$V_1(T, r) = F_1(T, r) - F_1(T, \infty) \quad (29)$$

The results of the fit to the free energy compared to the lattice data as well as the resulting potentials is shown in fig 3.

B. Results

Using the defined lattice potential from the previous section the methods of Section II can be applied. Do the previous results justify using the Kelbg potential to approximate the

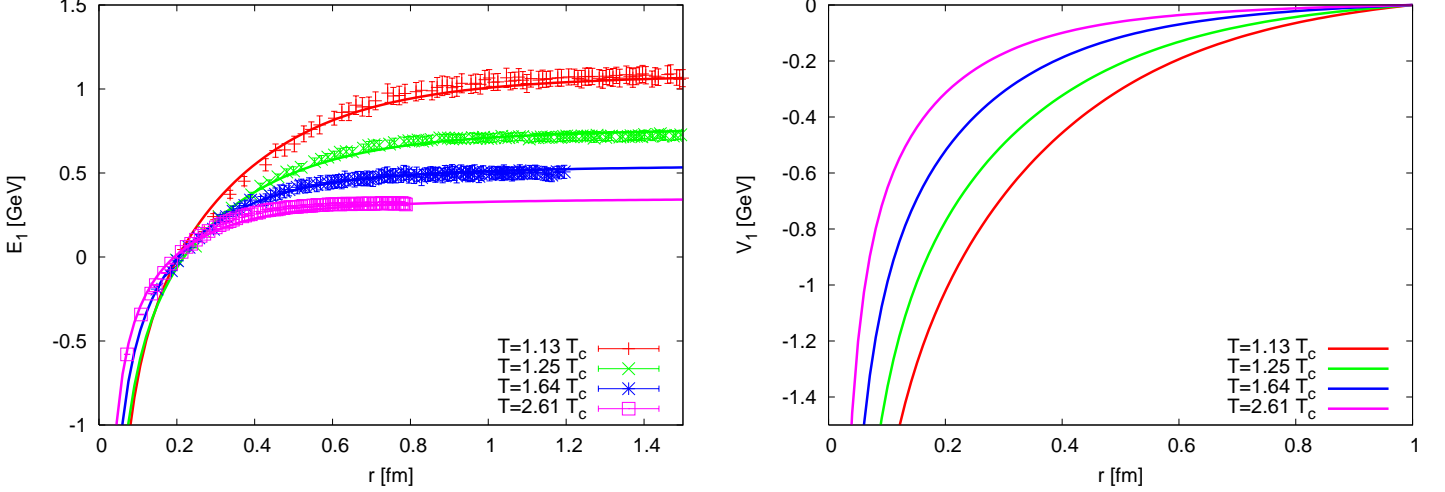


FIG. 3: Left: Lattice results for unquenched color singlet free energy compared to the parameterization in eq. 28. Right: Corresponding $Q\bar{Q}$ potentials from eq. 29.

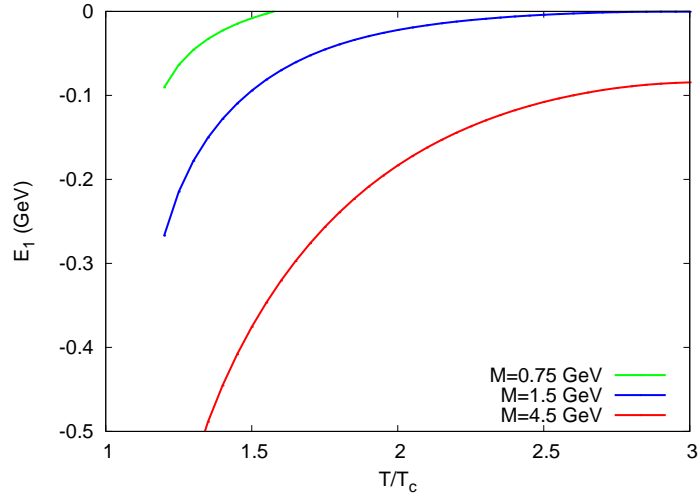


FIG. 4: Lowest $Q\bar{Q}$ bound state energy as a function of temperature.

effective $Q\bar{Q}$ potential? Well, since the divergent term in eq. 28 is the screened Coulomb term at small r , we may work in units where $|E_1(r, T)| < \frac{1}{r}$. The question then is whether or not β is sufficiently small in these units of the Bohr energy E_B . The answer is yes, since in the extreme case where the Bohr energy is the highest and the temperature is at the lowest (near T_c), we actually have $T \sim E_B$, where our results for the Coulomb case clearly show the Kelbg potential working well down to $T = 0.1E_B$. So we are confident that our methods will work well for the temperature range of interest.

In fig. 5 we show the results for $u_1(r)$ for charmonium and bottomonium (dotted blue and

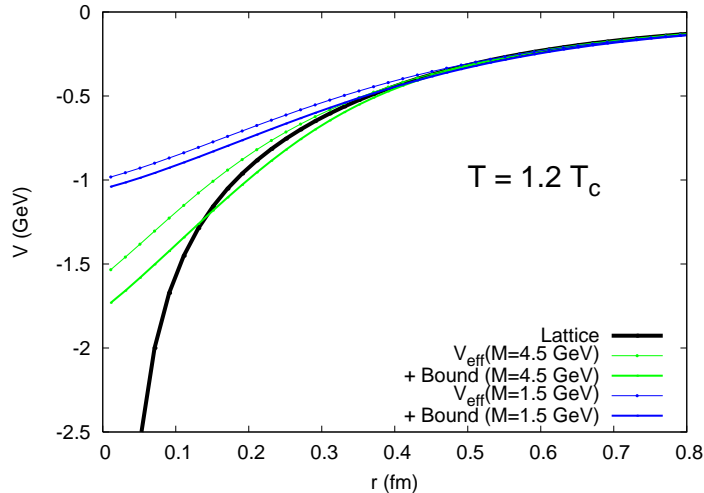


FIG. 5: Effective potential from the lattice data for charmonium and bottomonium at $T = 1.2T_c$. The dotted (upper) curves show u_1 and the solid (lower) curves show the result after the orthogonalization to the lowest bound state.

green lines respectively) at a temperature $T = 1.2T_c$. As in the Coulomb case the effective potential takes on a finite value at $r = 0$.

It is also possible to include the effect of the lowest bound state as was done in the Coulomb case. The wavefunction and lowest bound state energy was found using a shooting method. The result for the lowest bound state of charmonium, bottomonium and also a light quark bound state having reduced mass $M = 0.75$ GeV is shown in fig. 4. Also shown in fig. 5 as solid lines is the effective potential when the lowest bound state is included using the BPL formulation. At $T = 1.2T_c$ the effect of the bound state is to lower the potential by about 5% for charmonium and by about 15% for bottomonium. The effect is even smaller at higher temperatures.

In order for the results given above to be useful in future simulations we now quote some useful results for Kelbg like screened coulomb and linear potentials. We note that equation 19 can be integrated exactly in the case of a screened coulomb potential, $V(r) = \frac{-\alpha e^{\mu r}}{r}$ with the result:

$$u_1(r, \lambda) = \frac{-\alpha}{\lambda \mu r} \sqrt{\frac{\pi}{4}} e^{-\mu r} e^{(\mu \lambda)^2/4} \times \left[1 - e^{2\mu r} - 2 \operatorname{erf}\left(\frac{\mu \lambda}{2}\right) + \operatorname{erf}\left(\frac{\mu \lambda}{2} - \frac{r}{\lambda}\right) + e^{2\mu r} \operatorname{erf}\left(\frac{\mu \lambda}{2} + \frac{r}{\lambda}\right) \right] \quad (30)$$

and for a linear potential $V(r) = br$:

$$u_1(r, \lambda) = \frac{b\lambda^2}{3r} \times \left[1 + 3\frac{r^2}{\lambda^2} - \left(1 + \frac{r^2}{\lambda^2}\right)e^{-r^2/\lambda^2} + \frac{\sqrt{\pi}r}{2\lambda} \left(3 + 2\frac{r^2}{\lambda^2}\right) \left(1 - \operatorname{erf}\left(\frac{r}{\lambda}\right)\right) \right] \quad (31)$$

which can be used as an approximation to the *confinement* term in the lattice potential at small distances. However, the inclusion of bound states which are most prominent at low temperature and higher masses must be calculated numerically from eq. 22.

IV. CONCLUSIONS

We have used methods developed for treating effective potentials in electron-ion plasmas in order to generate potentials for quarkonium above deconfinement that properly take into account quantum effects and symmetry considerations. The nature of the potential changes at small distances ($r < 1fm$) and reaches a finite value at zero as is also seen in the Coulomb case. These effective potentials should be used in classical transport simulations as well as in molecular dynamic simulations of the quark-gluon plasma when Γ is sufficiently small.

-
- [1] E. V. Shuryak, arXiv:hep-ph/0608177.
 - [2] Edward V. Shuryak and Ismail Zahed, *Phys. Rev. C* 70, 021901 (2004).
 - [3] Edward V. Shuryak and Ismail Zahed, *Phys. Rev. D* 70, 054507 (2004).
 - [4] Boris A. Gelman, Edward V. Shuryak and Ismail Zahed, *Phys. Rev. C* 74 044908 (2006).
 - [5] Boris A. Gelman, Edward V. Shuryak and Ismail Zahed, *Phys. Rev. C* 74 044909 (2006).
 - [6] C. Young, E. Shuryak and D. Teaney, "Charmonium in strongly coupled Quark-Gluon Plasma", 2007
 - [7] O. Kaczmarek, F. Karsch, P. Petreczky and F. Zantow, *Nucl. Phys. B-Proc. Suppl.*, Vol. 129-130, March 2004, 560-562
 - [8] D. Hilton, N. March, A. R. Curtis, *Proc. Roy. Soc. A* **300**, 391 (1967).
 - [9] W. Ebeling and J. Ortner, *Physica Scripta* Vol. T75, 93-98, 1998
 - [10] A V Filinov, M Bonitz and W Ebeling, *J. Phys. A: Math. Gen.* 36(2003) 5957-5962
 - [11] W. D. Kraeft, D. Kremp, W. Ebeling, and G. Röpke, *Quantum Statistics of Charged Particle Systems*, 1986.
 - [12] D. M. Ceperley, *Reviews of Modern Physics* Vol. 67, No. 2, April 1995

- [13] F. Karsch, M. T. Mehr, and H. Satz, *Z. Phys. C.* **37**, 617(1988)
- [14] M. Le Bellac, *Thermal Field Theory*, p. 126-127, 1996